JOURNAL OF COMPUTATIONAL PHYSICS 96, 193–216 (1991)

Density-Scaling: A New Monte Carlo Technique in Statistical Mechanics

J. P. VALLEAU

Chemical Physics Theory Group,
Lash Miller Laboratories, University of Toronto, Toronto, Ontario, Canada M5S 1A1

Received August 30, 1990; revised February 21, 1991

We demonstrate the feasibility of using "umbrella sampling" to do Monte Carlo Markov-sampling runs each covering a substantial range of density: "density-scaling Monte Carlo," or DSMC. One can obtain in this way not only the usual canonical averages but also the relative free energy as a function of density. To test this it has been applied to systems for which there are some previous reliable results: the hard-sphere system and the restricted primitive model of 1:1 and 2:2 electrolytes. The method proves to be startlingly powerful in that very extensive results can be obtained with very few DSMC runs. An important further motivation is the prospect of using the technique to study phase transition regions.

1. MOTIVATION

In Monte Carlo computations in statistical mechanics, "umbrella sampling" implies sampling, in a single realization, the parts of configuration space relevant to a range of physical situations [1]. The sampling distribution will itself be non-physical, in the sense that it will not correspond to the ensemble distribution function for any one physical state. Instead it will be chosen arbitrarily to give adequate coverage of the relevant part of phase space for every state in the range addressed. The outstanding feature of such calculations is perhaps that one can then obtain the relative *free energies* of the system throughout the range of situations included. Unlike most other Monte Carlo free energy methods, this technique is not restricted to low-density systems [1, 2]. (Of course one obtains at the same time the usual mechanical quantities such as energy and correlation functions.)

The umbrella sampling technique has been used in a variety of ways. For example, a range of *models* can be studied by encompassing a range of parameters in a parametrized Hamiltonian [1–3] ("Hamiltonian-scaling Monte Carlo," or HSMC). This allows determination of the free energy for one model from that of another (for which the free energy may already be known from prior computations or in some other way)—e.g., the Lennard–Jones fluid from the "soft-sphere" model [1]. Another possibility is to cover a range of *temperatures* for a single Hamiltonian [1, 2, 4, 5] ("temperature-scaling Monte Carlo," or TSMC). In a different application, umbrella-sampling can be used to allow examination of physically-rare

0021-9991/91 $3.00

configurations in a system. For example, this allows the study of potentials of mean force in a system [6], and does so even for very strong forces such as those of the activation barrier regions of infrequent processes in the system [7]. In a similar way the relative stability of long-lived conformational states of molecules [8], and even of large or polymeric molecules [9], can be studied by finding and sampling along a path joining the relatively stable conformations.

A thermodynamic application of particular importance has been that of elucidating phase transition behaviour [2, 4, 5]. Where a transition has a critical point, this can be done by *mapping* the free energy A as a function of temperature T and concentration C. Such a map can be constructed by first obtaining the free energy along a reference isotherm at a supercritical temperature, using thermodynamic integration, HSMC, grand canonical methods, or in some other way. TSMC can then be used to obtain the temperature dependence at several concentrations C, resulting in a map of $A(T, C)$ (see Fig. 1). This map can then be analyzed to find the coexistence curve and the thermodynamics of the phase transition. Such a procedure has been carried out for several systems. An attractive feature is that the Monte Carlo sampling does not correspond to physical sampling of the model under consideration (since the sampling distribution is non-physical) and so the quasi-ergodic problems ordinarily encountered with conventional Monte Carlo computation near phase transitions may be avoided: in the coexistence region the samples correspond to the homogeneous system with its associated Van der Waal's loop.

Despite the success of the methods just described, they are inconvenient for some purposes. For example, one is really often merely seeking free energy and other thermodynamic and structural data on some model as a function of *density* at some single temperature, in which case temperature-scaling (TSMC) is not very helpful. Nor is it ideal for studies of first-order transitions, where the coexisting phases will be at the *same* temperature but have *different* densities. (The path between the phases in the scheme described earlier is by TSMC to the reference isotherm, along the reference isotherm to the density of the second phase and then back down to the coexistence temperature using TSMC once more (Fig. 1)—a long path for nearby states!) Furthermore, it is not applicable to freezing, since in that case there is no critical point.

It is clear that what is wanted is to do the Monte Carlo scaling in the *density* direction instead: "density-scaling Monte Carlo," or DSMC. It is not so obvious that this is possible, however. In the case of temperature-scaling (TSMC) the sampling demands are not too challenging: a change of temperature will correspond merely to a change in the relative probabilities of configurations of different energies. What is required is therefore only the sampling of a suitably broadened range of energies. If there is any substantial *density* change, on the other hand, the very nature of the configurations is seriously affected: the question is whether an appropriate sampling technique can be invented.

The rest of this paper is concerned with a successful attempt to do so. In this paper we consider only one-phase systems. The method is discussed in Section 2. In

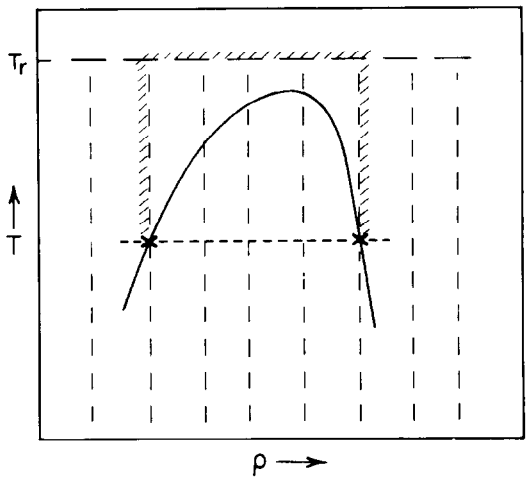

FIG. 1. Schematic representation of study of a phase transition using temperature-scaling. After determining the free energy A along a reference isotherm at some temperature T_r (heavy dashed line) by some method, TSMC is carried out at arbitrary densities (vertical dashed lines) to obtain a map of $A(T, \rho)$. The location of coexisting phases can then be determined at each temperature and the coexistence curve traced out. The method developed in the present paper, DSMC, seeks instead to obtain the relative free energies along an isotherm directly (horizontal line of short dashes) as a function of density. This would provide a direct link between coexisting phases (crosses) rather than by the long route (hatched path) required in the previous approach.

Sections 3 and 4 it is applied to two models and the results are compared with those obtained in quite different ways. The two models are the hard-sphere fluid over a wide range of density and the dilute primitive-model coulombic fluid. They are contrasting cases in that the structure of the former is determined entirely by the harshest of short-ranged forces, while for the latter the interesting features depend principally on the very long-ranged coulombic attractions and repulsions.

2. General Method

For simplicity the argument is developed for a system of N identical structureless particles; there is no difficulty about including internal energy modes or a mixture of components (see, e.g., Section 4). The intention is to find the relative free energies of the system over a range of density. The difference of Helmholtz free energy $\Delta A \equiv A_2 - A_1$ at two different densities ρ_2 and ρ_1 is given, for a (large) number N of particles and at a temperature T, by

$$\frac{\Delta A}{kT} = -\ln \frac{Q(N, V_2, T)}{Q(N, V_1, T)}, \tag{2.1}$$

where $\rho_1 = N/V_1$, $\rho_2 = N/V_2$. In this equation the configuration integral $Q(N, V_k, T)$ is given by

$$Q(N, V_k, T) \equiv \int_{(V_k)} d\mathbf{q}^N \exp(-\beta U(\mathbf{q}^N)), \tag{2.2}$$

where $\beta \equiv 1/k_B T$, $\mathbf{q}^N$ is the N-particle configuration $(\mathbf{q}_1, \mathbf{q}_2, ..., \mathbf{q}_i, ..., \mathbf{q}_N)$, and $U(\mathbf{q}^N)$ is the potential energy. Each position $\mathbf{q}_i$ is integrated, as indicated, over the volume V_k corresponding to the density ρ_k.

To estimate ΔA using (2.1) means estimating the ratio $Q(N, V_2, T)/Q(N, V_1, T)$. To estimate this ratio in a Monte Carlo procedure we must evidently generate a sample of configurations that includes the parts of configuration space that are important to both the numerator and denominator of the ratio. We would like to do so in a way that includes simultaneously, for some $V_1 = N/\rho_1$, regarded as a reference state, a substantial range of V_2's.

This sampling problem can be made more amenable by re-writing (2.2) in terms of *reduced* position vectors $\mathbf{r}_i$,

$$\mathbf{r}_i \equiv \mathbf{q}_i / L_k, \tag{2.3}$$

where $L_k^3 = V_k$. Then (2.2) becomes

$$Q(N, V_k, T) = V_k^N \int_{(1)} d\mathbf{r}^N \exp(-\beta U(\mathbf{r}^N, L_k)) \equiv V_k^N Q'(N, L_k, T), \tag{2.4}$$

where the final form defines a "reduced configuration integral" Q'. In (2.4), $U(\mathbf{r}^N, L_k)$ is just $U(\mathbf{q}^N)$, at the density N/L_k^3, expressed in terms of L_k and the reduced positions $\mathbf{r}^N$. In view of (2.4), (2.1) may be written

$$\frac{\Delta A}{NkT} + \ln \frac{V_2}{V_1} = \frac{\Delta A_{ex}}{NkT} = -\frac{1}{N} \ln \left\{ \frac{Q'(N, L_2, T)}{Q'(N, L_1, T)} \right\}. \tag{2.5}$$

In Q' each position $\mathbf{r}_i$ is of course integrated over *unit* volume, as indicated in (2.4), regardless of the density. (For example, in calculations on a bulk fluid it would be natural to use the (periodic) unit cube.) To obtain good estimates of the Q'-ratio in (2.5) requires the sampling of the configurations $\mathbf{r}^N$ to include those important to both the numerator and the denominator for each density of interest.

The sampling problem can thus be reduced to that of sampling N points in a unit periodic volume. *Each* configuration of these points will contribute to $Q'(N, L_k, T)$ for *every* density $\rho_k = N/L_k^3$. The formal aspects of such a procedure are easy to develop: Suppose the configurations $\mathbf{r}^N$ of the N points in their unit volume are generated in a Monte Carlo Markov-chain sampling procedure to belong to the sampling distribution $\pi(\mathbf{r}^N)$, and that we may choose a sampling distribution $\pi(\mathbf{r}^N)$

appropriate to the purpose we have outlined. Then (simply by inserting ratios identical to unity) we can evidently write

$$\frac{Q'(N, L_2, T)}{Q'(N, L_1, T)} \equiv \frac{\int_{(1)} d\mathbf{r}^N (\pi(\mathbf{r}^N)/\pi(\mathbf{r}^N)) \exp(-\beta U(\mathbf{r}^N, L_2))}{\int_{(1)} d\mathbf{r}^N (\pi(\mathbf{r}^N)/\pi(\mathbf{r}^N)) \exp(-\beta U(\mathbf{r}^N, L_1))} \times \frac{\int_{(1)} d\mathbf{r}^N \pi(\mathbf{r}^N)}{\int_{(1)} d\mathbf{r}^N \pi(\mathbf{r}^N)}$$
$$\equiv \frac{\langle \exp(-\beta U(\mathbf{r}^N, L_2))/\pi(\mathbf{r}^N) \rangle_\pi}{\langle \exp(-\beta U(\mathbf{r}^N, L_1))/\pi(\mathbf{r}^N) \rangle_\pi}, \tag{2.6}$$

where $\langle \cdots \rangle_\pi$ indicates an average over the distribution $\pi(\mathbf{r}^N)$.

Since the sampling distribution $\pi(\mathbf{r}^N)$ must *include* the region of the reduced configuration space $\mathbf{r}^N$ relevant to the canonical distribution for each density ρ_k of the range to which π is "appropriate," canonical averages can also be obtained at *all* such densities. For example the canonical average configurational energy $\langle U \rangle_{\rho_k, \text{can}}$ can immediately be written

$$\langle U(q^N) \rangle_{\rho_k, \text{can}} \equiv \frac{\int_{(1)} d\mathbf{r}^N U(\mathbf{r}^N, L_k) \exp(-\beta U(\mathbf{r}^N, L_k))}{\int_{(1)} d\mathbf{r}^N \exp(-\beta U(\mathbf{r}^N, L_k))}$$
$$\equiv \frac{\int_{(1)} d\mathbf{r}^N (\pi(\mathbf{r}^N)/\pi(\mathbf{r}^N))\, U(\mathbf{r}^N, L_k) \exp(-\beta U(\mathbf{r}^N, L_k))}{\int_{(1)} d\mathbf{r}^N (\pi(\mathbf{r}^N)/\pi(\mathbf{r}^N)) \exp(-\beta U(\mathbf{r}^N, L_k))} \times \frac{\int_{(1)} d\mathbf{r}^N \pi(\mathbf{r}^N)}{\int_{(1)} d\mathbf{r}^N \pi(\mathbf{r}^N)}$$
$$= \frac{\langle U(\mathbf{r}^N, L_k) \exp(-\beta U(\mathbf{r}^N, L_k))/\pi(\mathbf{r}^N) \rangle_\pi}{\langle \exp(-\beta U(\mathbf{r}^N, L_k))/\pi(\mathbf{r}^N) \rangle_\pi}. \tag{2.7}$$

The data for pair correlation functions can be obtained similarly.

Formally this is straightforward. The challenge is actually to *find* a sampling distribution $\pi(\mathbf{r}^N)$ which is "appropriate" in the sense of allowing reliable estimation of the Q'-ratio of (2.5) and (2.6) over a substantial range of relative density $\rho_2 - \rho_1$. It is clear that this sampling problem is not trivial, however, because the important configurations at different densities will correspond to *markedly* different reduced configurations $\mathbf{r}^N$. (In this regard density-scaling (DSMC) is considerably more challenging than temperature-scaling (TSMC).)

To see this, imagine a typical configuration (in real space, $\mathbf{q}^N$) of the system, and consider the separation, q_{nn}, between the pair of particles *nearest to each other* in such a configuration. This nearest-neighbour distance will be determined by the harsh short-ranged repulsive force between the particles, and it will vary only rather little with the density. But this means that the typical *reduced* nearest-neighbour separation, $r_{nn} = q_{nn}/L_k$, will therefore be quite *strongly* dependent on the density, since L_k is proportional to $\rho_k^{-1/3}$. If we are to sample the reduced configurations appropriate to a range of densities, therefore, we must ensure that the sampled configurations exhibit an appropriate range of reduced nearest-neighbour separations r_{nn}.

This implies a general approach to finding an appropriate sampling distribution

$\pi(\mathbf{r}^N)$, namely to ensure that we can impose an appropriate distribution of $\mathbf{r}_{nn}$. This suggests the form

$$\pi(\mathbf{r}^N) = w(r_{nn})\, p(\mathbf{r}^N), \tag{2.7}$$

with $w(r_{nn})$ chosen to satisfy this condition; $p(\mathbf{r}^N)$ must ensure that, as well, an appropriate range of energies is sampled, and so on, and will reflect the intermolecular forces under consideration. In the examples that follow, sampling distributions of the general form (2.7) have been successful.

The Monte Carlo runs were carried out in the familiar way. A trial move was attempted at each step for one of the N points, chosen at random; the trial move was uniformly distributed in a cube of length δ about the initial position. The distribution $\pi(\mathbf{r}^N)$ is ensured by accepting the move with probability $\min(1, \pi_j/\pi_i)$, where π_j is the probability of the new state and π_i that of the initial state, as given by $\pi(\mathbf{r}^N)$. The "maximum step size" δ was chosen to give a reasonable convergence rate. As described below, $\pi(\mathbf{r}^N)$ can be written as an expression involving one or two parameters. These were adjusted to give a suitable sampling distribution during short preliminary runs which also served to relax the system from the arbitrary initial configuration.

3. The Hard-Sphere System

For the hard-sphere system density-scaling is especially simple conceptually, but particularly difficult computationally. In terms of our present notation the model is defined by

$$\begin{aligned} U(\mathbf{r}^N, L_k) &= 0, \qquad r_{nn} > \sigma/L_k \\ &= \infty, \qquad r_{nn} < \sigma/L_k, \end{aligned} \tag{3.1}$$

where r_{nn} is still the (reduced) separation of the pair of points nearest to each other in the system, σ is the hard-sphere diameter, and the density $\rho_k = N/L_k^3$. It follows that a particular configuration $\mathbf{r}^N$ will make an *equal* contribution, proportional to $1/\pi(\mathbf{r}^N)$, to $Q'(N, L_k, T)$ for *all* densities ρ_k small enough that $r_{nn} > \sigma/L_k$, and zero for all larger densities. This makes density-scaling easy to understand for the hard-sphere case (and allows easy data-collection).

Since for this model the only property of the configuration $\mathbf{r}^N$ on which the contributions depend is the reduced nearest-neighbour r_{nn}, it is natural to try a sampling distribution $\pi(\mathbf{r}^N)$ which depends solely on that separation, i.e.,

$$\pi(\mathbf{r}^N) = w(r_{nn}), \tag{3.2}$$

where $w(r_{nn})$ is some function of r_{nn}. The results reported in this paper were obtained using this simple form. The sampling was done for N points in a periodic unit cube. To study the densities ρ in some range $\rho_1 \leqslant \rho \leqslant \rho_2$, configurations with

$r_{nn} < \sigma/L_1$ give *no* contribution, so one can set $w(r_{nn}) = 0$ for such configurations. Otherwise the form of $w(r_{nn})$ must be chosen to force the occurrence of the larger values of r_{nn} (up to $r_{nn} > \sigma/L_2$), for otherwise such values would occur only rarely: i.e., for hard spheres $w(r_{nn})$ will be an increasing function of r_{nn} in the range $\sigma/L_1 < r_{nn} < \sigma/L_2$. (For $r_{nn} > \sigma/L_2$ it is sufficient to set $w(r_{nn}) = w(\sigma/L_2)$.)

For a chosen range $\rho_2 - \rho_1$ of density a satisfactory *numerical* form of $w(r_{nn})$ can easily be generated by trial and error: what is required is fairly uniform sampling (in r_{nn}^3) over the range of interest. This was tried successfully, but it proved more convenient to work with an *analytic* form for $w(r_{nn})$ involving only one or two parameters. Some of the results reported here were obtained using (in $\sigma/L_1 < r_{nn} < \sigma/L_2$)

$$w(r_{nn}) \propto \exp(aNr_{nn}^3), \tag{3.3}$$

which can be adjusted, through a, to give a suitable uniformity of sampling over the density range. This provides the required strong dependence on r_{nn} and was satisfactory at the lower densities. However, it does not always capture the required curvature adequately; this can be corrected by including a quadratic pre-exponential factor adjusted by a second parameter b:

$$w(r_{nn}) \propto \left(1 + b\left(r_{nn} - \frac{\sigma}{L_1}\right)\left(r_{nn} - \frac{\sigma}{L_2}\right)\right) \exp(aNr_{nn}^3). \tag{3.4}$$

To cover very large ranges in a single run one might want to develop still more

TABLE I

Hard-Sphere DSMC Runs

Density range	$w(r_{nn})$		No. Confs.	
0.4—0.5	$a = 448$,	$b = 0$	1×10^7	
0.5—0.6	$a = 526$,	$b = 0$	5×10^6	
	$a = 536$,	$b = 150$	3×10^6	
	$a = 530$,	$b = 320$	3×10^6	(a)
0.6—0.7	$a = 660$,	$b = 300$	3×10^6	
	$a = 660$,	$b = 350$	3×10^6	(a)
0.7—0.8	$a = 796$,	$b = 320$	5×10^6	(a)
0.8—0.9	$a = 1025$,	$b = 405$	5×10^6	
	$a = 1028$,	$b = 405$	8×10^6	(a)

Note. In some density ranges extra runs were carried out as the programme was refined (e.g., to include pair data); these parallel data were pooled. The column "$w(r_{nn})$" gives the parameters used in the sampling function (3.4); "No. Confs." is the number of MC configurations used in the averages; (a) indicates runs in which pair correlation data were collected.

flexible sampling functions. The alternative, of covering a large range with overlapping realizations of more modest ranges, was followed here.

Results are reported for samples of 108 particles in the moderate to dense fluid range $0.4 \leqslant \rho\sigma^3 \leqslant 0.9$, covered in five equal overlapping ranges (0.4 to 0.5, 0.5 to 0.6, etc.). This was arbitrary; it could certainly have been covered in fewer runs without difficulty. The weighting of the sampling by $w(r_{nn})$ is fairly dramatic: for example, in the DSMC run covering the range $0.8 \leqslant \rho\sigma^* \leqslant 0.9$ the value of $w(r_{nn})$ at the high-density and was some 4×10^{44} greater than at the lower! Nevertheless the sampling proceeds smoothly enough. In some cases the results for a density range were pooled from shorter runs (see Table I).

One could extract thermodynamic data at as many densities as one wished, in the sampled range. In the data reported here they were extracted for the set of reduced densities $\rho\sigma^3$ separated by 0.004—i.e., at 26 densities in each DSMC run. The collection of data for the pair correlation functions is relatively time-consuming, so they were collected at fewer densities, those separated by 0.02—i.e., at six densities in each run.

The procedure just described led to the Helmholtz free energy results shown in Fig. 2. Of course, as is clear from (2.5), DSMC runs give only *relative* free energies

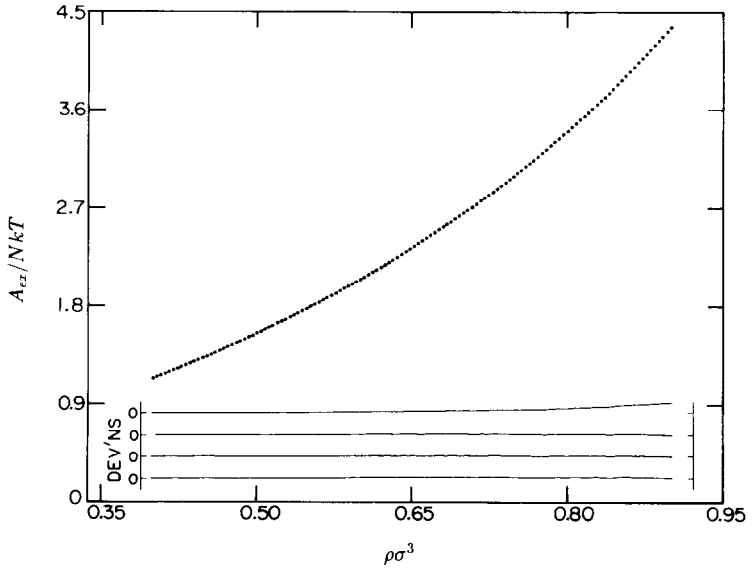

FIG. 2. Reduced excess free energy of hard spheres obtained by DSMC on a system of 108 particles. The values have been extracted at intervals of 0.004 in $\rho\sigma^3$. The four lines in the lower part show the deviations of the DSMC points from, top to bottom, the sixth-order virial expansion (using the known virial coefficients up to B_7), the eighth-order virial (by fitting the two additional coefficients B_8 and B_9), the Padé approximation of Hoover and Ree, and the Carnahan–Starling approximation. Each is on the same scale as the main graph, but with the zeros shifted to separate them from each other and the axis. Only the sixth-order virial shows any systematic deviation.

in the density range covered. Since our five runs overlapped at $\rho\sigma^3 = 0.5$, 0.6, 0.7, and 0.8 to form a continuous series, they immediately give the relative free energy over the whole range $0.4 \leqslant \rho\sigma^3 \leqslant 0.9$. But for the special case of hard spheres it is possible to fix the *absolute* values of the excess free energy quite accurately, as follows: The virial coefficients for hard spheres are known [10, 11] with good accuracy up to the seventh, B_7, and one expects this many terms to give a good description of the thermodynamic behaviour up to densities well within the range we covered. The observed excess reduced free energy relative to that at $\rho^* = \rho\sigma^3 = 0.4$ was therefore fitted, for our lower densities, to the expression

$$\frac{A_{ex}(\rho\sigma^3) - A_{ex}(0.4)}{NkT} = C + \sum_{j=2}^{7} B_j \rho^{j-1}/(j-1) \tag{3.5}$$

by a least-squares adjustment of C, keeping the known values of the (pressure) virial coefficients B_j. Since the sum shown in (3.5) is the absolute value of the excess free energy at moderate densities, this determines $A_{ex}(0.4)/NkT = -C$ from our data. Using least squares in the range $0.4 \leqslant \rho\sigma^3 \leqslant 0.5$ gave $A_{ex}(0.4)/NkT = 1.1305$; the range $0.4 \leqslant \rho\sigma^3 \leqslant 0.6$ gave 1.1312; χ^2 per degree of freedom was 10^{-6} in either case, assuming constant probable relative error. The value must therefore be close to 1.131, and the values of A_{ex}/NkT plotted in Fig. 2 are the *absolute* values obtained by adding 1.131 to our observed values relative to $\rho\sigma^3 = 0.4$.

Another, more direct, way of obtaining $A_{ex}(0.4)$ is simply to estimate it directly from the sixth-order density expansion. This gives $A_{ex}(0.4)/NkT = 1.1308$. It is gratifying that this is so close to the first estimate, which depended essentially on the shape of the density-dependence of the observed DSMC free energies.

Hoover and Ree developed a Padé approximation for the excess free energy of hard spheres [12], based on the known virial coefficients up to B_6, and it is believed to be very accurate. (It gives the value 1.1310 for the reduced excess free energy at $\rho\sigma^3 = 0.4$, by the way.) If plotted on Fig. 2a it would disappear under the DSMC points, so instead the discrepancy of the latter and the Padé is plotted below, but the deviations are scarcely visible. Indeed they are far closer than there is any reason to expect: the average difference of the DSMC points from the Padé is -0.0024, and the root-mean-square deviation of the DSMC free energy from the Padé is only 3×10^{-3}, i.e., of the order of 0.1%! This speaks well for the smoothness of the DSMC results (the extraordinary agreement of those results to the Padé must itself be partly fortuitous, however, since for one thing the latter should really apply to the thermodynamic limit rather than to a finite system).

This figure also shows the discrepancy between the DSMC results and the virial series using all the known coefficients (i.e., up to the sixth-order term $B_7\rho^6/6$): they diverge above $\rho\sigma^3 = 0.7$. If two further terms are added—those of B_8 and B_9—they can be adjusted (by least squares) to fit the data. This gives $B_8/B_2^7 = (-6.57 \pm 0.63) \times 10^{-3}$ and $B_9/B_2^8 = (+8.73 \pm 0.43) \times 10^{-3}$; the mean square deviation is 3×10^{-6}. It is interesting that B_8 appears to be negative, because it has long been realized that there must be one or more negative virial coefficients for hard

spheres, in view of the existence of the fluid–solid phase transition. The above cannot be considered a reliable determination of these virial coefficients, however, in spite of the excellent fit, because of the very large negative correlation coefficient (-0.997) for the two parameters.

Another expression for the excess free energy of hard spheres, believed to be very accurate, was given by Carnahan and Starling [13] by combining some integral-equation-theory results. According to this

$$\frac{A_{ex}}{NkT} = \frac{4\eta - 3\eta^2}{(1-\eta)^2} \tag{3.6}$$

where $\eta = \pi\rho\sigma^3/6$. This also fits the DSMC results very closely, as can be seen by the graph of deviations in Fig. 2; the root-mean-square deviation is again 3×10^{-3}.

Pair correlation functions were collected in the $\rho\sigma^3$ range 0.5–0.9 at intervals of 0.02. Figure 3 shows, as an example, the six correlation functions in the range 0.5–0.6 obtained in a single DSMC run: the gradual change of shape is obvious. Also shown for comparison are the results at 0.6 obtained from the low-density end of the DSMC run for the adjoining range 0.6–0.7.

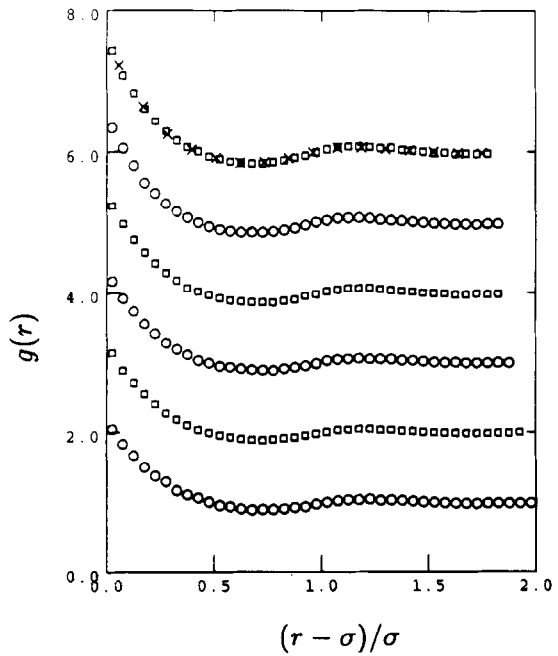

FIG. 3. Pair correlation functions for hard spheres at six densities, obtained from a single DSMC run. The functions at successive densities are displaced upwards by 1.0. At the highest density, the crosses show results from the lowest-density point of the DSMC run covering the higher range 0.6–0.7, to emphasize the reliability.

The pressure can be calculated from the pair correlation functions $g(r)$ in the usual way [14],

$$\frac{p_{ex}}{\rho kT} \equiv \frac{p}{\rho kT} - 1 = \frac{2\pi}{3} \rho\sigma^3 g(\sigma), \tag{3.7}$$

where $g(\sigma)$ is the value of $g(r)$ at contact, $r = \sigma$; $g(\sigma)$ was obtained by fitting a cubic polynomial in $(r - \sigma)$ to (usually) eight values of $g(r)$. In Fig. 4 the results are compared with the Padé pressure approximation of the Ree and Hoover [10]. The agreement is reasonable, although they tend to be slightly below the Padé (which, in view of the free energy results, we know to be very accurate here). This probably means that the pair function data should have been collected on a finer grid (but they would then be noisier) and that a better extrapolation function was needed, presumably one with greater curvature near contact—but it is not known what function would be appropriate, so the results are always likely to be biassed by the choice. This difficulty of evaluating the pressure from $g(r)$ is a general problem where the particles have harsh repulsive forces.

Of course, there is in principle no need to use the pair-function route (3.5) to p_{ex}

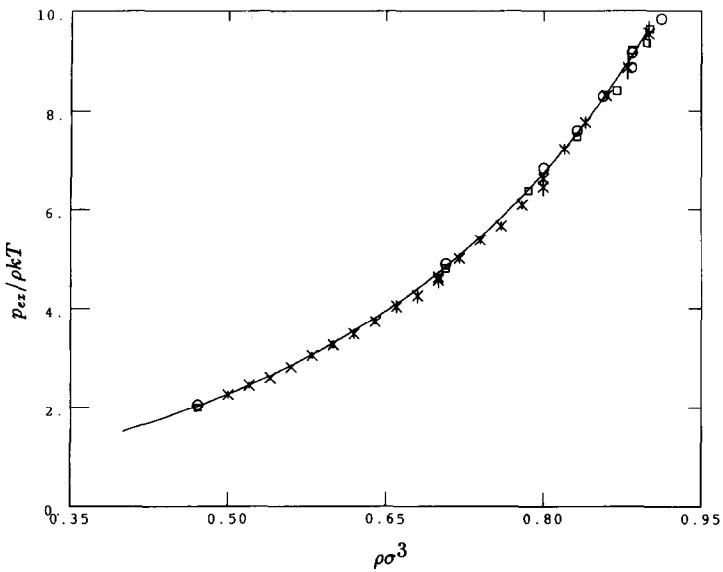

FIG. 4. The crosses show the reduced excess pressures (3.5) obtained by cubic extrapolations of the pair functions obtained by DSMC. The bars show twice the standard deviation of that fit. For comparison is shown the Padé approximation [10] of Ree and Hoover, which in view of the free energy results must be very accurate. The circles show some results due to Alder and Wainwright [22] and the squares results due to Wood and Jacobson [23].

in the case of DSMC, since the pressure could instead be obtained from the observed density dependence of the free energy through

$$p_{ex} = -\left.\frac{\partial A_{ex}}{\partial V}\right|_{T,N} = \frac{\rho^2}{N}\left.\frac{\partial A_{ex}}{\partial \rho}\right|_{T}. \tag{3.8}$$

This was calculated by four-point numerical differentiation [15] of the free-energy results, using a 0.012 reduced-density grid (except for two points at each extreme of the density, where a finer grid of 0.008 had to be used). Unlike the pressures based on (3.5) these will not be much biassed in the data extraction process; on the other hand, we must expect such results obtained by numerical differentiation to be very noisy. The resulting pressures are shown in Fig. 5. The *average* discrepancy between these results and the Padé is, of course, negligible: 0.008, while the standard deviaton is 0.08. As expected their accuracy is better than that of the pressures obtained from $g(\sigma)$, although their apparent precision is only moderate in view of the numerical differentiation.

These pressure data obtained by differentiation of the free energy can again be fitted to an eighth-order virial expansion (up to the B_9 term), using the known coefficient values up to B_7. This yields a standard deviation of 0.07 in $p_{ex}/\rho kT$, and the values $B_8/B_2^7 = (-5.6 \pm 4.1) \times 10^{-3}$ and $B_9/B_2^8 = +(8.1 \pm 2.4) \times 10^{-3}$. It is gratifying that these agree within their large uncertainties with the coefficients derived from the more accurate free energy data; however, the two sets of data are not really independent.

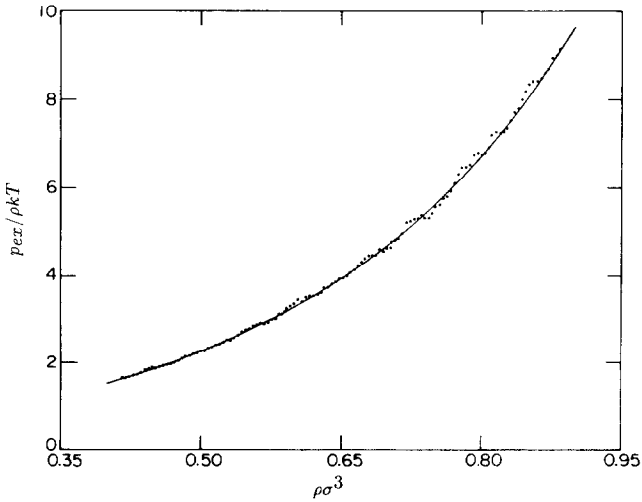

FIG. 5. Reduced excess pressure obtained by numerical differentiation of the DSMC free energies, again compared with the Padé result.

In view of the excellence of the Carnahan and Starling formula (3.6) and of the Padé of Hoover and Ree, in representing the DSMC results, there seems no point in tabulating the data.

4. Restricted Primitive Model Coulomb System

The "primitive model" consists of charged hard spheres immersed in a continuum dielectric. It is a basic model for the theory of electrolytes and in plasma physics and is especially interesting at low densities. Although this model also has a hard core, it represents at low densities an opposite extreme to the hard-sphere system, since its behaviour is dominated by the weak and long-ranged coulomb forces.

Now the model is defined by specifying that the energy at a density $\rho_k = N/L_k^3$ corresponding to a configuration $\mathbf{r}^N$ in reduced coordinates is given by

$$\begin{aligned} U(\mathbf{r}^N, L_k) &= \frac{e^2}{\varepsilon L_k} \sum_{i<j} \frac{Z_i Z_j}{r_{ij}}, \qquad && r_{nn} > \frac{\sigma}{L_k} \\ &= \infty, && r_{nn} < \frac{\sigma}{L_k}, \end{aligned} \tag{4.1}$$

where ε is the continuum dielectric constant, $-e$ is the electronic charge, $Z_i\,|e|$ is the charge on ion i, and r_{ij} is the *reduced* separation of ions i and j. (This assumes that the hard-core diameter σ is the same for all the pairs of ions—i.e., we study the "restricted" primitive model, RPM—but could easily be generalized.)

Once again the configurations were sampled in a unit periodic cube. The densities were low enough that the choice between minimum-image and Ewald energy approximation is irrelevant; the former was used. The sampling distribution took the form

$$\pi(\mathbf{r}^N) = w(r_{nn}) \exp\left(-\frac{\beta e^2}{\varepsilon \sigma} r_{nn} \sum_{i<j} \frac{Z_i Z_j}{r_{ij}} \right). \tag{4.2}$$

TABLE II

RPM DSMC Runs

Electrolyte	Density range	$w(r_{nn})$		No. Confs.
1:1	0.05–0.15	$a' = -375$,	$b' = 3600$	6×10^6
	0.13–0.23	$a' = -1145$,	$b' = 7500$	6×10^6
	0.21–0.31	$a' = -1850$,	$b' = 12000$	6×10^6
2:2	0.02–0.12	$a' = 785$,	$b' = 1280$	1×10^7
	0.02–0.12	$a' = 788$,	$b' = 1284$	6×10^6
	0.10–0.20	$a' = 365$,	$b' = 0$	8×10^6
	0.20–0.30	$a' = -35$,	$b' = 5800$	1×10^7

Note. The column "$w(r_{nn})$" gives the parameter used in the sampling distribution (4.2, 3).

The rationale for this form was as follows. At a given density ρ_k there will, of course, almost always be unlike ions very close to contact; in the reduced description this says that r_{nn} will be very close to its minimum σ/L_k. Then (cf. (4.1) and (4.2)) in the limit $r_{nn}=\sigma/L_k$ the energy distribution will be canonical for the density ρ_k—but a configuration with a given r_{nn} will make a substantial contribution only to a narrow range of density, and of σ/L, so the form (4.2) should ensure adequate energy-sampling. The reported results confirm that this is the case.

The term $w(r_{nn})$ is required to force the range of r_{nn} corresponding to the desired density range. In the reported results we used the form

$$\begin{aligned} &w(r_{nn})=0, \qquad \text{if} \quad r_{nn}<\sigma/L_1 \\ &w(r_{nn}) \propto \left(1+b'\left(r_{nn}-\frac{\sigma}{L_1}\right)\left(r_{nn}-\frac{\sigma}{L_2}\right)\right)\exp(-a'r_{nn}), \qquad \sigma/L_1<r_{nn}<\sigma/L_2, \end{aligned} \tag{4.3}$$

adjusting a' and b' to give fairly uniform sampling over the density range of interest. In (4.3), L_1 and L_2 correspond to the minimum and maximum densities studied, according to $\rho L^3=N$. For $r_{nn}>\sigma/L_2$, $w(r_{nn})$ was set to decay with r_{nn} so that a sufficient but limited range of r_{nn} was sampled (the precise form used depended on the sign of a', but the results are not sensitive to it).

We report results for $|Z_i|=1$ and with values of $\varepsilon\sigma T$ corresponding to 1:1 and 2:2 electrolytes, with $\sigma=4.25\text{Å}$ and 4.2Å, respectively, in a solvent of dielectric con-

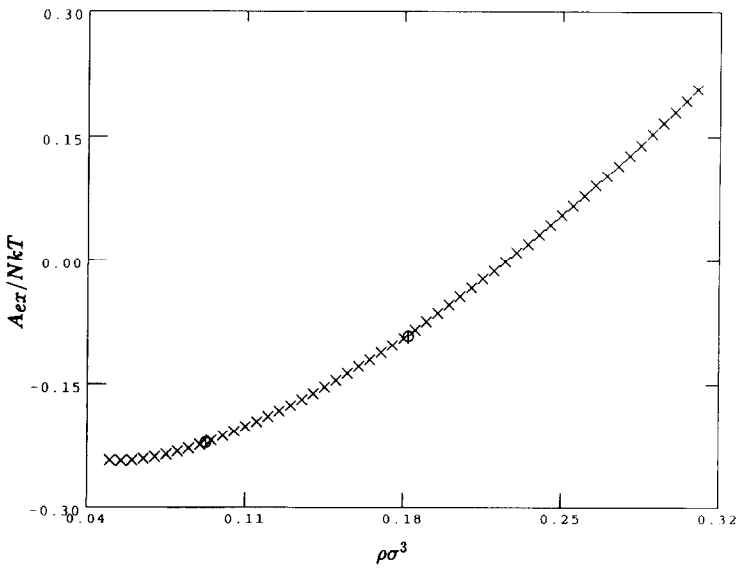

FIG. 6. Reduced excess free energy A_{ex}/NkT for the 1:1 RPM as a function of reduced density, obtained by DSMC. The two circles refer to the MSS results: at the lower concentration was used to fix the zero for the DSMC results: the other tests their accuracy.

stant 78.5 at 25°C. There is extensive previous work on these systems by conventional canonical and grand canonical Monte Carlo, with which the present DSMC results can be compared. (If one thinks of these systems, instead, as being 1:1 ionic plasmas in a vacuum, with the above ion sizes, the temperatures correspond to 23420°K and 5855°K, respectively.)

The 1:1 system was studied by DSMC for systems of 128 particles, the 2:2 for 64; details of the runs are recorded in Table II. The 1:1 system was studied over $0.05 \leqslant \rho\sigma^3 \leqslant 0.31$ (i.e., $0.54M \leqslant C \leqslant 3.35M$) in three overlapping DSMC runs, the 2:2 over $0.02 \leqslant \rho\sigma^3 \leqslant 0.30$ ($0.224M \leqslant C \leqslant 3.36M$), again in three overlapping ranges. The thermodynamic data was collected on a grid of densities $\rho\sigma^3$ separated by 0.005 and consisted of relative free energies and reduced configurational energies at each density; the osmotic pressures and ionic activity coefficients are obtained by numerical differentiation of the free energy data. Pair correlation data were collected in some of the runs.

The resulting thermodynamic data for the 1:1 system is collected in Table III. The reduced excess free energy is shown in Fig. 6. In each run the relative values of the free energy are obtained. By using the overlapping density regions of the runs, these are easily combined into relative free energies over the whole range $0.05 \leqslant \rho\sigma^3 \leqslant 0.31$. (In doing this matching, several data points were used in the substantial overlap regions between the runs, unlike the hard-sphere case where a single common density was used in each case.) However, the free energy relative to

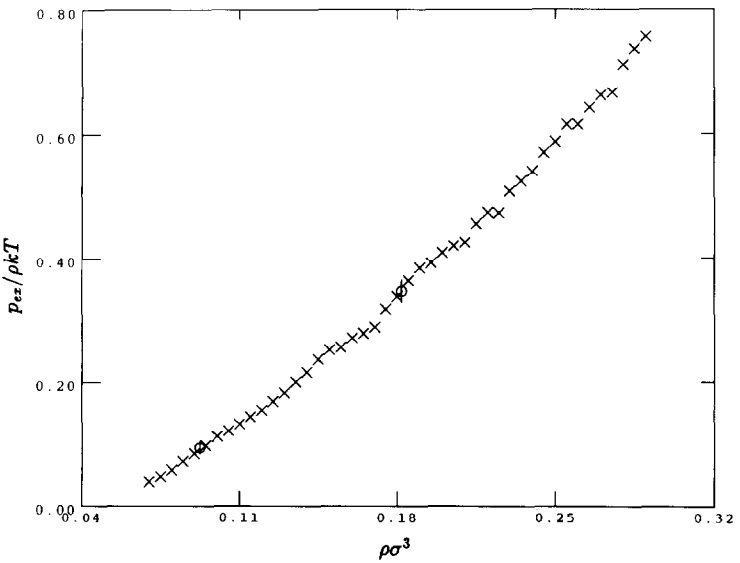

FIG. 7. Reduced excess pressure obtained by numerical differentiation of the DSMC free energy (to be interpreted as the excess osmotic coefficient of the electrolyte). The circles were obtained by canonical MC techniques; their error bars are ± 2 standard deviations.

TABLE III

1:1 DSMC Results

$\rho\sigma^3$	A_{ex}/NkT	U/NkT	$P_{ex}/\rho kT$	$\log(\gamma)$
0.050	-0.243200	-0.466100	---	---
0.055	-0.243808	-0.478900	---	---
0.060	-0.243326	-0.492400	---	---
0.065	-0.241304	-0.505000	---	---
0.070	-0.239022	-0.514500	0.039590	-0.199500
0.075	-0.236078	-0.524000	0.047648	-0.188500
0.080	-0.232490	-0.533800	0.058412	-0.174100
0.085	-0.228696	-0.543000	0.072358	-0.156400
0.090	-0.224379	-0.549400	0.084525	-0.139900
0.095	-0.219183	-0.557100	0.097672	-0.121600
0.100	-0.213796	-0.565300	0.112437	-0.101400
0.105	-0.208292	-0.570900	0.120966	-0.087400
0.110	-0.202176	-0.577000	0.131994	-0.070200
0.115	-0.196222	-0.586000	0.143960	-0.052300
0.120	-0.189794	-0.593500	0.154424	-0.035400
0.125	-0.183258	-0.601200	0.168811	-0.014500
0.130	-0.176351	-0.606800	0.182821	0.006400
0.135	-0.169124	-0.612600	0.200333	0.031200
0.140	-0.161620	-0.618100	0.215775	0.054100
0.145	-0.153567	-0.622700	0.236844	0.083200
0.150	-0.145543	-0.629000	0.252502	0.106900
0.155	-0.136773	-0.633200	0.256329	0.119500
0.160	-0.128276	-0.637800	0.271637	0.143300
0.165	-0.120460	-0.643000	0.279056	0.158500
0.170	-0.111601	-0.649600	0.289351	0.177700
0.175	-0.102716	-0.651100	0.318008	0.215200
0.180	-0.093810	-0.656800	0.338533	0.244700
0.185	-0.084060	-0.661600	0.363890	0.279800
0.190	-0.074062	-0.667300	0.384505	0.310400
0.195	-0.063632	-0.669700	0.392826	0.329100
0.200	-0.053656	-0.672400	0.409506	0.355800
0.205	-0.043822	-0.677900	0.420569	0.376700
0.210	-0.033218	-0.683900	0.425994	0.392700
0.215	-0.022552	-0.688000	0.455501	0.432900
0.220	-0.012758	-0.690900	0.473541	0.460700
0.225	-0.001611	-0.692900	0.472961	0.471300
0.230	0.009699	-0.697400	0.508116	0.517800
0.235	0.019826	-0.702900	0.524143	0.543900
0.240	0.031383	-0.705700	0.539799	0.571100
0.245	0.042954	-0.709900	0.570259	0.613200
0.250	0.054807	-0.713700	0.587447	0.642200
0.255	0.066316	-0.715000	0.615122	0.681400
0.260	0.078205	-0.720400	0.615488	0.693600
0.265	0.091006	-0.723300	0.642126	0.733100
0.270	0.102303	-0.726000	0.662200	0.764500
0.275	0.114775	-0.727500	0.666192	0.780900
0.280	0.127280	-0.731000	0.711771	0.839000
0.285	0.139847	-0.735200	0.737249	0.877000
0.290	0.153095	-0.739500	0.756728	0.909800
0.295	0.166339	-0.741900	---	---
0.300	0.179497	-0.747300	---	---
0.305	0.193097	-0.746600	---	---
0.310	0.206905	-0.751600	---	---

Note. Reduced density $\rho\sigma^3$, reduced excess free energy, reduced configurational energy, excess osmotic coefficient, and the logarithm of the mean ionic activity coefficient. The last two quantities depend on numerical differentiation of the free energy.

the hard-sphere fluid was previously [16] obtained at a few concentrations using "multi-stage sampling" (MSS, an inefficient precursor of umbrella sampling). By adding to those MSS results the excess free energy of the hard-sphere fluid, we obtain the absolute value of the excess free energy. Doing this for the $1.0M$ MSS result, using the Carnahan–Starling formula [13] to estimate the hard-sphere contribution, we can find the absolute value of the excess free energies over our density range. It is these values that are given in Table III and Fig. 6. Figure 6 shows the MSS point used for calibration ($\rho\sigma^3 = 0.925$), and also a MSS point for $1.968M$ ($\rho\sigma^3 = 0.1820$) which is seen to agree perfectly with the variation shown by the DSMC results.

Differentiation of the excess free energy leads to

$$\frac{p_{ex}}{\rho kT} = \frac{p}{\rho kT} - 1 = \frac{\rho}{NkT}\frac{\partial A_{ex}}{\partial \rho}\bigg|_T \tag{4.4}$$

$$\log \gamma_{\pm} \equiv \frac{\mu}{kT} - \frac{\mu_{id}}{kT} = \frac{A_{ex}}{NkT} + \frac{p_{ex}}{\rho kT}. \tag{4.5}$$

Under the McMillan–Mayer interpretation [17] of this model, p in (4.4) is the osmotic pressure, and $p_{ex}/\rho kT$ is the excess osmotic coefficient of the electrolyte. We described above how we could assign an absolute value to our excess free energies, which in turn, according to (4.5), gives us the values of the mean ionic activity coefficient at each density. Of course, we must expect the results to be

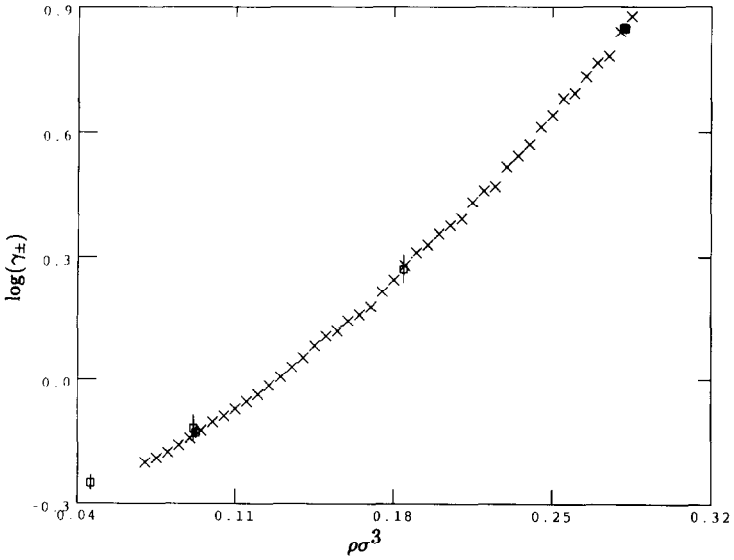

FIG. 8. Logarithm of the mean ionic activity coefficient of the 1:1 RPM. The squares show grand canonical results (with ± 2 standard deviations.)

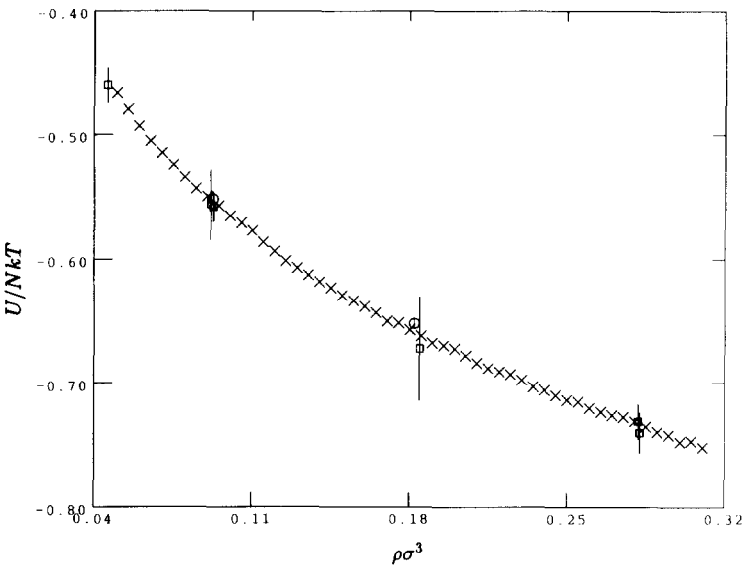

FIG. 9. Reduced configurational energy of the 1:1 RPM obtained in the DSMC runs. The circles and squares show respectively canonical and grand canonical results (with error bars of ± 2 standard deviations).

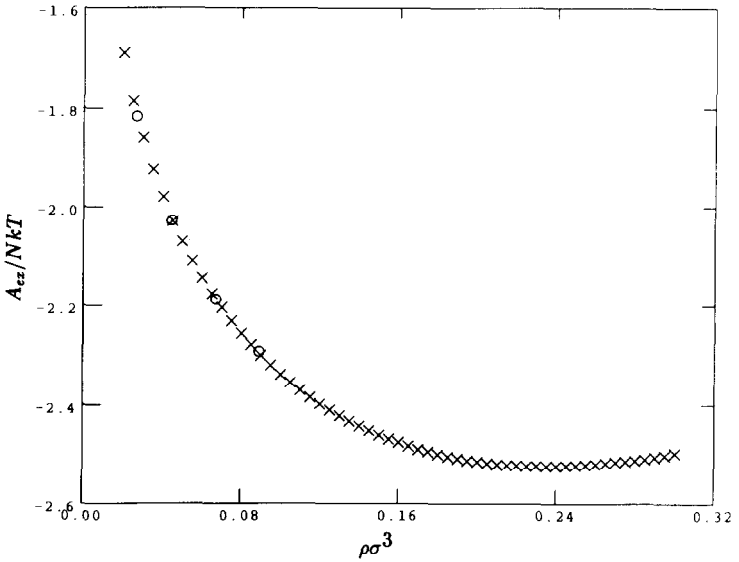

FIG. 10. Reduced excess free energy of the 2:2 RPM obtained by DSMC. The circles correspond to a Padé based on a fit to grand-canonical activity coefficients.

TABLE IV

2:2 DSMC Results

$\rho\sigma^3$	A_{ex}/NkT	U/NkT	$p_{ex}/\rho kT$	$\log(\gamma)$
0.020	-1.690000	-2.386800	---	---
0.025	-1.785526	-2.502500	---	---
0.030	-1.860345	-2.578900	---	---
0.035	-1.923744	-2.648700	---	---
0.040	-1.979032	-2.700400	-0.406184	-2.385200
0.045	-2.027931	-2.757200	-0.408651	-2.436500
0.050	-2.069288	-2.810800	-0.403303	-2.472500
0.055	-2.108716	-2.865600	-0.400504	-2.509200
0.060	-2.142992	-2.902300	-0.401049	-2.544000
0.065	-2.175565	-2.943300	-0.394405	-2.569900
0.070	-2.204102	-2.974200	-0.390778	-2.594800
0.075	-2.230994	-3.011000	-0.380873	-2.611800
0.080	-2.255450	-3.045000	-0.376414	-2.631800
0.085	-2.278020	-3.076900	-0.372578	-2.650500
0.090	-2.299040	-3.109500	-0.370582	-2.669600
0.095	-2.318959	-3.143200	-0.355348	-2.674300
0.100	-2.337874	-3.171000	-0.350358	-2.688200
0.105	-2.353291	-3.196600	-0.341863	-2.695100
0.110	-2.369387	-3.226400	-0.327119	-2.696500
0.115	-2.384305	-3.250900	-0.326582	-2.710800
0.120	-2.397791	-3.275000	-0.312472	-2.710200
0.125	-2.410088	-3.298800	-0.299678	-2.709700
0.130	-2.421519	-3.322000	-0.288076	-2.709500
0.135	-2.432547	-3.343900	-0.278029	-2.710500
0.140	-2.442462	-3.367400	-0.276602	-2.719000
0.145	-2.451536	-3.386800	-0.262206	-2.713700
0.150	-2.460843	-3.407500	-0.242339	-2.703100
0.155	-2.468753	-3.430700	-0.241706	-2.710400
0.160	-2.475294	-3.448200	-0.237019	-2.712300
0.165	-2.482741	-3.466900	-0.215699	-2.698400
0.170	-2.490297	-3.489300	-0.215577	-2.705800
0.175	-2.495065	-3.507300	-0.196680	-2.691700
0.180	-2.500332	-3.527500	-0.164383	-2.664700
0.185	-2.505159	-3.545600	-0.169210	-2.674300
0.190	-2.508977	-3.559000	-0.139188	-2.648100
0.195	-2.513227	-3.576200	-0.126976	-2.640200
0.200	-2.515142	-3.593000	-0.122146	-2.637200
0.205	-2.518284	-3.626100	-0.087356	-2.605600
0.210	-2.520872	-3.639900	-0.073719	-2.594500
0.215	-2.521924	-3.648000	-0.057155	-2.579000
0.220	-2.522202	-3.662200	-0.020002	-2.542200
0.225	-2.523594	-3.683700	-0.018611	-2.542200
0.230	-2.523330	-3.694300	-0.022124	-2.545400
0.235	-2.523813	-3.707300	0.001957	-2.521800
0.240	-2.523901	-3.722700	0.002647	-2.521200
0.245	-2.523473	-3.734100	0.019826	-2.503600
0.250	-2.522919	-3.748400	0.046005	-2.476900
0.255	-2.521954	-3.764500	0.066256	-2.455600
0.260	-2.520234	-3.775500	0.093398	-2.426800
0.265	-2.518434	-3.789200	0.098238	-2.420100
0.270	-2.516076	-3.804200	0.105287	-2.410700
0.275	-2.514675	-3.820300	0.114704	-2.399900
0.280	-2.512264	-3.834500	0.136814	-2.375400
0.285	-2.509725	-3.845700	---	---
0.290	-2.505960	-3.858300	---	---
0.295	-2.502339	-3.868400	---	---
0.300	-2.497939	-3.885200	---	---

somewhat noisy due to the numerical differentiation. The derivative in (4.4) was estimated by four-point numerical differentiation using a grid of 0.010 in $\rho\sigma^3$.

Figure 7 shows the excess osmotic coefficients obtained in this way. For comparison are shown some values obtained from the pair correlation functions at contact estimated by extrapolation of canonical Monte Carlo results [18]. Figure 8 shows the activity coefficient (4.5), along with several values derived previously [19] from grand canonical Monte Carlo calculations. The agreement is very satisfactory.

The configurational internal energy is evaluated during the DSMC runs. Figure 9 shows the results, along with the results of canonical [18] and grand canonical [19] Monte Carlo experiments.

Similar comparisons are possible for the 2:2 case. In this case the absolute value of the excess free energy at a single concentration can be fixed using the values derived by Graham and Valleau [5], based on a fit to the grand canonical chemical potential data. Then the DSMC results yield the excess free energy at each concentration; it is these values that appear in Table IV and Fig. 10. The figure shows the DSMC results and also several values given by the fit mentioned above [5].

It is of interest that the DSMC runs behave smoothly up to at least $3.3M$, because conventional grand-canonical simulations appeared to become erratic at lower concentrations [19]. It seems likely that some "quasi-ergodicity" trap is being avoided by the use of our non-physical sampling distribution.

The osmotic coefficient is shown in Fig. 11. The canonical results [20] shown

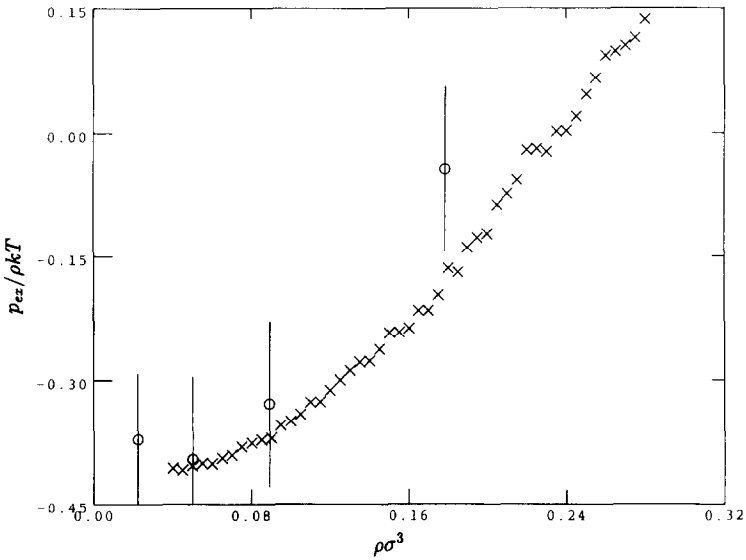

FIG. 11. Excess osmotic coefficient for the 2:2 RPM. The canonical results (circles with ± 2 standard deviations) are unreliable due to the impossibility of reliable extrapolation of the pair functions. The DSMC results are, of course, somewhat noisy due to the numerical differentiation.

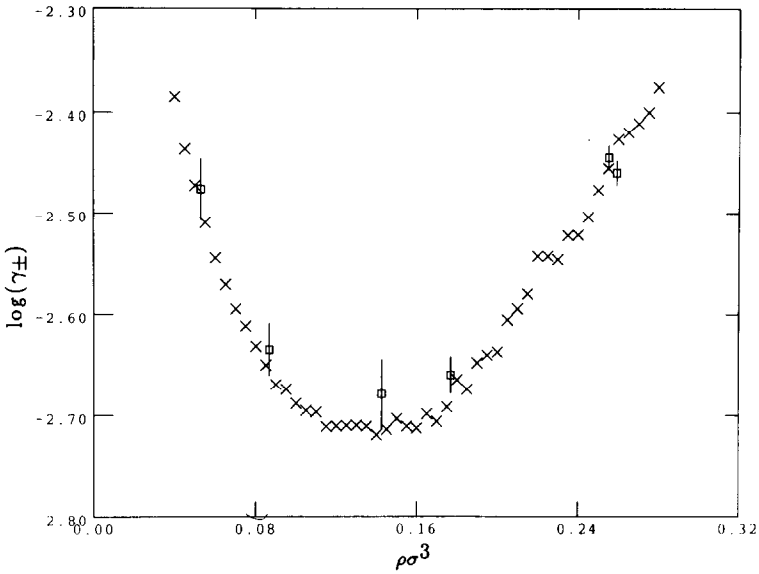

FIG. 12. Logarithm of the mean ionic activity coefficient obtained by DSMC (crosses). The squares show grand canonical results (± 2 standard deviations).

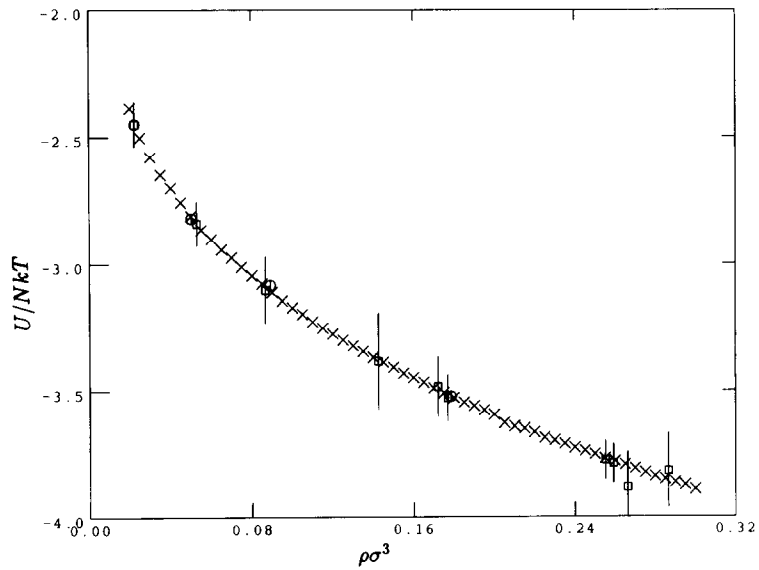

FIG. 13. Reduced configurational energy for 2:2 RPM obtained by DSMC (crosses). The circles are canonical results and the squares grand canonical (± 2 standard deviations).

there agree rather poorly. This is not surprising, since they could only be obtained by extrapolation to contact of the pair correlation functions. The pair functions rise so dramatically near contact for these systems that reliable extrapolation is out of the question. (For that reason these canonical results were never published.) Figure 12 shows the activity coefficients, along with grand canonical results [19] for systems with a similar number of particles. The agreement is moderate; except at the lower concentrations we are, however, into the region where grand canonical results appeared somewhat erratic, as mentioned above.

The DSMC configurational energy results are shown in Fig. 13 and are, again, compared with canonical [20] and grand canonical [19] results.

Figure 14 shows by way of example pair correlation functions obtained in a single DSMC run. It is rather satisfying to see the changes of shape and the contraction of the pair functions as the density is increased, revealed from within a single Monte Carlo run. The results are entirely consistent with previous canonical Monte Carlo results [20, 21].

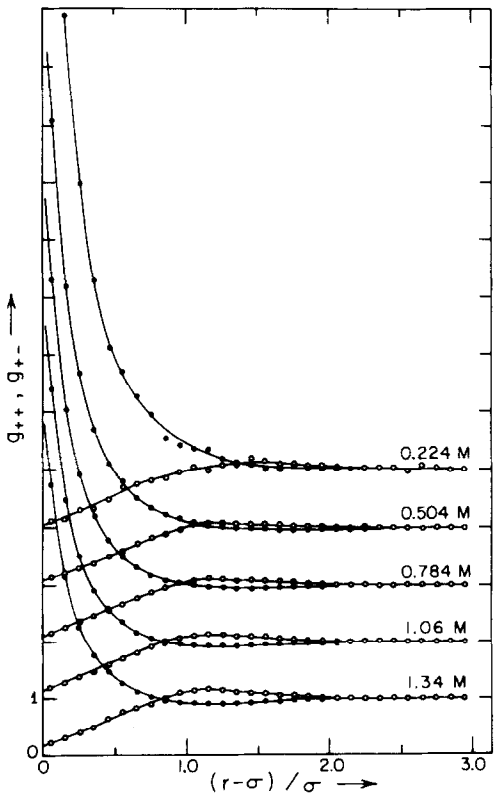

FIG. 14. Pair correlation functions for like and unlike ion pairs at several densities obtained in a single DSMC run. The functions at successive densities are displaced upwards by 1.0.

5. CONCLUSION

This paper demonstrates the feasibility of using umbrella sampling to obtain thermodynamic and structural information over a substantial range of density in a single Monte Carlo run. One obtains not only canonical averages of mechanical quantities, but also relative free energies. One can extract data for as many densities as one wishes, in the range covered. Thus one gets large quantities of data; this is especially useful in that they can then readily be manipulated to take advantage of thermodynamic relations; a good example is the numerical differentiation used in the present cases to derive pressures and activity coefficients.

The method is inherently efficient, in that each configuration sampled contributes to the averages at several different densities. The results reported in the paper are by far more extensive than previously obtained for these systems, but for the 1:1 coulombic system ($0.54M$–$3.3M$) and the 2:2 ($0.22M$–$3.4M$) these results were obtained in three DSMC runs. The hard-sphere system (126 states in the range $(0.4 < \rho\sigma^3 < 0.9)$ was done in five DSMC runs, though fewer could conveniently have been used.

Fortunately, it proves to be quite straightforward to find an appropriate umbrella sampling distribution $\pi(\mathbf{r}^N)$ by adjusting a couple of parameters in a suitable chosen function.

On an Apollo DN10000 computer the 2:2 RPM runs required about 25 min per 10^6 configurations, when pair function data was not collected. Pair function data increased that time to over an hour, however, simply because a lot of sums must be stored. Evidently it is thrifty to avoid this unless structural data is actually wanted; taking advantage of the methods demonstrated above, we can get all the conventional canonical simulations).

Both of the models studied had hard cores, but there is no reason to expect any difficulty with soft repulsions. (There will no longer be a sharp cutoff of $w(r_{nn})$ at a value of r_{nn} fixed by the minimum density, of course.) A test of the Lennard–Jones system is underway. The extension to non-central forces and to more complicated molecules requires investigation.

As discussed in Section 1, an immediate attraction of the technique is the possibility of studying phase transitions. The special feature of interest is that one hopes that by using this quite non-physical sampling one can avoid the quasi-ergodicity normally associated with simulations near phase transitions. This immunity has been evidenced in several TSMC investigations previously [1, 2, 4, 5], but DSMC should offer a more direct and effective way of exploring the phase transition region. One hopes in this way to explore at a single temperature the density range encompassing phase separations. Some applications along those lines are well underway and will be reported elsewhere.

ACKNOWLEDGMENT

The financial support of the Natural Sciences and Engineering Research Council is gratefully acknowledged.

REFERENCES

1. G. M. TORRIE AND J. P. VALLEAU, *J. Comput. Phys.* **23**, 187 (1977).
2. G. M. TORRIE AND J. P. VALLEAU, *J. Chem. Phys.* **66**, 1402 (1977).
3. The description "Hamiltonian-scaling Monte Carlo" was introduced in "Equilibrium Ensembles and Their Computer Realization: The Gibbsian Programme," J. P. VALLEAU, International Symposium on Ludwig Boltzmann, Rome, February 1989. The technique had already been applied several times, however.
4. K.-C. NG, J. P. VALLEAU, G. M. TORRIE, AND G. N. PATEY, *Mol. Phys.* **38**, 781 (1979).
5. I. S. GRAHAM AND J. P. VALLEAU, *J. Phys. Chem.* **94**, 7894 (1990).
6. G. N. PATEY AND J. P. VALLEAU, *J. Chem. Phys.* **63**, 2334 (1975).
7. Some examples are in J. CHANDRASEKHAR, S. F. SMITH, AND W. L. JORGENSEN, *J. Am. Chem. Soc.* **107**, 154 (1985); C. PANGALI, M. RAO, AND B. J. BERNE, *J. Chem. Phys.* **21**, 2982 (1979); G. RAVISHANKAR, M. MEZEI, AND D. L. BEVERIDGE, *Faraday Symp. Chem. Soc.* **17**, 79 (1982).
8. A very nice example is in D. W. REBERTUS, B. J. BERNE, AND D. CHANDLER, *J. Chem. Phys.* **70**, 3395 (1979).
9. See for example, M. MEZEI, P. K. MEHROTA, AND D. L. BEVERIDGE, *J. Am. Chem. Soc.* **107**, 2239 (1985); W. L. JORGENSEN, *J. Phys. Chem.* **87**, 5304 (1983).
10. F. H. REE AND W. G. HOOVER, *J. Chem. Phys.* **40**, 939 (1964).
11. F. H. REE AND W. G. HOOVER, *J. Chem. Phys.* **46**, 4181 (1967).
12. W. G. HOOVER AND F. H. REE, *J. Chem. Phys.* **49**, 3609 (1968).
13. N. F. CARNAHAN AND K. E. STARLING, *J. Chem. Phys.* **51**, 635 (1969).
14. See W. W. WOOD, in *Physics of Simple Liquids*, edited by H. N. V. Temperley, J. S. Rowlinson, and G. S. Rushbrooke (North-Holland, Amsterdam, 1968), Eq. (50), p. 115.
15. Explicitly, by the second form of the numerical estimate of the slope appearing in Eq. (13–9), H. MARGENAU AND G. M. MURPHY, *Mathematics of Physics and Chemistry*, 2nd ed. (Van Nostrand, Princeton, NJ, 1956).
16. J. P. VALLEAU AND D. N. CARD, *J. Chem. Phys.* **57**, 5457 (1972).
17. An elegant review of the McMillan–Mayer formulation is found in an article by H. L. FRIEDMAN AND W. D. T. DALE, *Statistical Mechanics, Part A: Equilibrium Techniques*, edited by B. J. Berne (Plenum, New York, 1977).
18. D. N. CARD AND J. P. VALLEAU, *J. Chem. Phys.* **52**, 6232 (1970).
19. J. P. VALLEAU AND L. K. COHEN, *J. Chem. Phys.* **72**, 5935 (1980).
20. D. N. CARD, Thesis, University of Toronto, 1972 (unpublished).
21. J. P. VALLEAU, L. K. COHEN, AND D. N. CARD, *J. Chem. Phys.* **72**, 5942 (1980).
22. B. J. ALDER AND T. E. WAINWRIGHT, *J. Chem. Phys.* **33**, 1439 (1960); see also Ref. [10].
23. W. W. WOOD, F. R. PARKER, AND J. D. JACOBSON, *Nuovo Cimento Suppl.* **9**, 133 (1958); see also Ref. [14].